



# THE UNIVERSITY *of* EDINBURGH

## Edinburgh Research Explorer

### **Prediction of intramuscular fat content and shear force in Texel lamb loins using combinations of different X-ray computed tomography (CT) scanning techniques**

**Citation for published version:**

Clelland, N, Bunger, L, McLean, KA, Knott, S, Matthews, KR & Lambe, NR 2018, 'Prediction of intramuscular fat content and shear force in Texel lamb loins using combinations of different X-ray computed tomography (CT) scanning techniques' Meat Science, vol. 140, pp. 78-85. DOI: 10.1016/j.meatsci.2018.03.003

**Digital Object Identifier (DOI):**

[10.1016/j.meatsci.2018.03.003](https://doi.org/10.1016/j.meatsci.2018.03.003)

**Link:**

[Link to publication record in Edinburgh Research Explorer](#)

**Document Version:**

Peer reviewed version

**Published In:**

Meat Science

**Publisher Rights Statement:**

© 2018 Elsevier Ltd. All rights reserved.

**General rights**

Copyright for the publications made accessible via the Edinburgh Research Explorer is retained by the author(s) and / or other copyright owners and it is a condition of accessing these publications that users recognise and abide by the legal requirements associated with these rights.

**Take down policy**

The University of Edinburgh has made every reasonable effort to ensure that Edinburgh Research Explorer content complies with UK legislation. If you believe that the public display of this file breaches copyright please contact [openaccess@ed.ac.uk](mailto:openaccess@ed.ac.uk) providing details, and we will remove access to the work immediately and investigate your claim.



1        **Prediction of intramuscular fat content and shear force in Texel lamb loins using**  
2        **combinations of different x-ray computed tomography (CT) scanning techniques**

3  
4    **N. Clelland<sup>1\*</sup>, L. Bunger<sup>1</sup>, K.A. McLean<sup>1</sup>, S. Knott<sup>2</sup>, K. Matthews<sup>3</sup> and N.R. Lambe<sup>1</sup>**

5  
6    *<sup>1</sup>Animal Breeding and Genetics, Animal and Veterinary Sciences group, Scotland's Rural*  
7    *College, West Mains Road, Edinburgh, EH9 3JG, United Kingdom*

8    *<sup>2</sup>Institute of Evolutionary Biology, School of Biological Sciences, University of Edinburgh,*  
9    *Ashworth Laboratories, West Mains Road, Edinburgh, EH9 3JT, UK*

10    *<sup>3</sup>English beef and lamb executive, Agriculture and Horticulture Development Board,*  
11    *Stoneleigh Park, Kenilworth, Warwickshire, CV8 2TL.*

12  
13    \*Address for correspondence:

14    Scotland's Rural College

15    Roslin Institute Building

16    Edinburgh

17    EH25 9RG

18    United Kingdom

19    Tel: +44131 651 9293

20    Email:Neil.Clelland@sruc.ac.uk

21

22

23

24

25

## 26 **Abstract**

27 Computed tomography (CT) parameters, including spiral computed tomography scanning  
28 (SCTS) parameters, intramuscular fat (IMF) and mechanically measured shear force were  
29 derived from two previously published studies. Purebred Texel (n = 377) of both sexes,  
30 females (n = 206) and intact males (n = 171) were used to investigate the prediction of IMF  
31 and shear force in the loin. Two and three dimensional CT density information was available.  
32 Accuracies in the prediction of shear force and IMF ranged from  $R^2$  0.02 to  $R^2$  0.13 and  $R^2$   
33 0.51 to  $R^2$  0.71 respectively, using combinations of SCTS and CT scan information. The  
34 prediction of mechanical shear force could not be achieved at an acceptable level of accuracy  
35 employing SCTS information. However, the prediction of IMF in the loin employing  
36 information from SCTS and additional information from standard CT scans was successful,  
37 providing evidence that the prediction of IMF and related meat eating quality (MEQ) traits  
38 for Texel lambs *in vivo* can be achieved.

39

40 **Keywords:** spiral x-ray computed tomography, lamb, meat quality, intramuscular fat.

41

## 42 **1. Introduction**

43 Computed tomography (CT) is a non-invasive, diagnostic tool initially developed for use in  
44 human medicine to improve the imaging of soft tissue structures and assist in diagnosing  
45 conditions or diseases not directly associated with bone structure. Over the last few decades  
46 CT has been adopted for use in animal breeding and is now routinely used in selective  
47 breeding programs for sheep in the UK to accurately estimate carcass composition of live  
48 animals. More recently, the prediction of aspects of meat quality (MQ) such as intramuscular  
49 fat levels (IMF), fatty acid profiles and tissue composition have been investigated both *in*  
50 *vivo* and post mortem in meat producing species (Font-i-Furnols, Brun, Tous, & Gispert,

51 2013; Kongsro & Gjerlaug-enger, 2013; L. Bünger, J.M. Macfarlane, N. R. Lambe, J.  
52 Conington, K. A. McLean, K. Moore, 2011; Prieto et al., 2010). The basic principle of CT is  
53 the measurement of the spatial distribution of any physical quantity. Offering greater contrast  
54 in the imaging of soft tissue to that seen in conventional radiography (Kalender, 2006). The  
55 first method of image capture most commonly used is ‘single-slice’ scanning. During single-  
56 slice scanning, x-rays are used to generate cross-sectional, two-dimensional images of the  
57 selected region of a subject. Each image is produced by rotation of the x-ray tube 360° around  
58 the subject. Attenuation of radiation through the tissues can then be measured, with  
59 differences indicating different tissue densities.

60

61 Advances in scanning technology have resulted in the development of contiguous scanning  
62 procedures such as spiral CT scanning (SCTS), capable of producing a series of images in a  
63 single contiguous scan at intervals of as little as 0.6 mm apart. The advantage is that multiple  
64 images can be acquired faster, at reduced intervals, resulting in increased information  
65 acquisitions in less time. Recent studies provide evidence that muscle density information  
66 from single or multiple CT scans in sheep, can provide moderately accurate predictions of  
67 IMF content *in vivo*. Prediction accuracies range from  $R^2 = 0.33$  to 0.68 using several  
68 approaches including various CT parameters (Clelland et al., 2014; Karamichou, Richardson,  
69 Nute, McLean, & Bishop, 2006; Lambe et al., 2008; Lambe, McLean, et al., 2010; J. M.  
70 Macfarlane, 2006). The aim of this study was to investigate any gains in the prediction of  
71 IMF content and shear force in the loins of Texel sheep that may be achieved by utilizing the  
72 wealth of information that relatively new SCTS techniques may provide.

73

74

75

## 76 **2. Materials and Methods**

### 77 *2.1. Experimental animals*

78 The CT parameters, including SCTS parameters, IMF and shear force in the loin were  
79 derived from two previously-published studies. The first of these studies (Exp. 1), was  
80 conducted over two years (2003 to 2004) and investigated the use of various *in vivo*  
81 measurement techniques (ultrasonography, video image analysis and CT), to predict carcass  
82 and meat quality in purebred Texel (n = 240) and Scottish Blackface (n = 233) lambs. The  
83 full study and methods are detailed in Lambe et al. (2008). The second study (Exp. 2) was  
84 conducted in 2009 and investigated the genotypic effects of the Texel muscling quantitative  
85 trait loci (TMQTL) on carcass and meat quality in purebred Texel lambs (n = 137). Full  
86 details are published in Lambe et al. (2010). The combination of these data from Exp. 1 and  
87 Exp. 2 comprised data from pure-bred Texel lambs (n = 377) of both sexes, females (n = 206)  
88 and intact males (n = 171). Lambs were reared to weaning as either singles (n = 184), twins  
89 (n = 168) or artificially hand reared (n = 25). Mean age at CT was 132 d (SD 21.1, range 91-  
90 202 d); with mean live weight 35.3kg (SD 4.9, range 20-49kg). Lambs were CT scanned pre-  
91 slaughter using a Siemens Somatom Esprit scanner. All lambs were lightly sedated  
92 (Rompun<sup>®</sup>, Bayer animal health, Bayer plc., Newbury, UK) at a dose of 0.1-0.2mg xylazine  
93 hydrochloride/kg body weight, then secured in a purpose-built cradle before being CT-  
94 scanned.

95

### 96 *2.2. Single-slice and spiral x-ray CT measurements and image analysis*

97 A series of spiral CT images at intervals of 8mm were selected from the loin region of each  
98 lamb. The first image was taken where the transverse process of the 7<sup>th</sup> lumbar vertebra  
99 appears and the last image in the series where the transverse process of the 1<sup>st</sup> lumbar  
100 vertebra is no longer visible (Fig.1a). Two-dimensional cross-sectional single-slice scans

101 were also used, taken at two defined anatomical positions, through the top of the leg at the  
102 ischium bone (ISC), and through the chest at the 8<sup>th</sup> thoracic vertebra (TV8), details of the  
103 images used and the location are presented in Fig. 1b.

104

105 **Insert Figure 1 Here**

106

107 This two dimensional method of scanning at these particular anatomical sites (including an  
108 additional scan at the 5<sup>th</sup> lumbar vertebra, which was not used in this study), is currently used  
109 in UK terminal sire breeding programs to provide accurate predictions of fat and muscle  
110 weights in the carcass. This method, defined as ‘reference’ scanning (L. Bünger, J.M.  
111 Macfarlane, N. R. Lambe, J. Conington, K. A. McLean, K. Moore, 2011), optimizes the  
112 number of images required to be taken across the body of the sheep while maximizing the  
113 accuracy of estimations for carcass traits. Images were produced with a resolution of 512 x  
114 512 pixels with a 450mm field of view, producing images with a pixel size of 0.77mm<sup>2</sup> in  
115 two dimensions. Spiral images were produced at the same resolution and field of view at  
116 intervals of 8mm, producing images with a voxel size of 6.2mm<sup>3</sup>.

117 Automated analyses were performed on the images produced, to separate carcass from non-  
118 carcass tissues (Glasbey & Young, 2002), and calculate the density of each pixel in  
119 Hounsfield units (HU), the standard quantitative scale for describing radiodensity. In the final  
120 segmented image each pixel was allocated to fat, muscle or bone using image thresholding  
121 techniques (Mann, Young, Glasbey, & McLean, 2003). The thresholds in Hounsfield units  
122 (HU) defined for the CT scanner (Siemens Somatom Esprit single slice) were Fat = -174 to -  
123 12HU, Muscle = -10 to 92HU and Bone = 94HU and above, based on previous calibration  
124 trials. Areas (mm<sup>2</sup>) and average densities (HU) of muscle and fat in each two dimensional  
125 image were calculated, as well as standard deviations of the density values allocated to each

126 tissue. Combining all pixels allocated as either fat or muscle enabled the use of a novel  
127 average ‘soft tissue density’ and standard deviation. The SCTS images were used to calculate  
128 weighted average densities of muscle, fat and soft tissue (average tissue density, in each  
129 individual scan image, weighted for tissue area in that image and averaged across all images  
130 in the spiral scan series). Volumes of each tissue ( $\text{mm}^3$ ) were also calculated. The resulting  
131 SCTS parameters included; weighted muscle and fat densities and relating standard  
132 deviations, weighted soft tissue densities and standard deviation, and calculated muscle and  
133 fat volumes ( $\text{mm}^3$ ). The CT parameters measured from the two dimensional reference scans  
134 in the ISC and TV8 regions were muscle density, fat density and related standard deviations,  
135 as well as the soft tissue densities and standard deviations of soft tissue densities. Muscle area  
136 and fat area tissue measurements ( $\text{mm}^2$ ) were also calculated for each of the reference scan  
137 images. Total CT predicted carcass fat (PrCfat), as a measure of subcutaneous and  
138 intermuscular fat in the entire carcass, was also predicted using a breed-specific prediction  
139 equation developed from previous research (Macfarlane et al., 2006):

$$140 \text{PrCfat}(kg) = (-2236 + (LW \times 80.26) + (ISCFA \times 0.21) + (LV5FA \times 0.19) + \\ 141 (TV8FA \times 0.221))/1000$$

142 Where PrCfat is the CT predicted weight of subcutaneous and intermuscular fat (kg), LW is  
143 live weight at CT scanning, ISCFA is the area of pixels allocated as fat in the scan image  
144 taken at the ischium ( $\text{mm}^2$ ), LV5FA is the area of pixels allocated as fat in the scan image  
145 taken at the 5<sup>th</sup> lumbar vertebra ( $\text{mm}^2$ ) and TV8FA is the area of pixels allocated as fat in the  
146 scan image taken at the 8<sup>th</sup> thoracic vertebra. Details, acronyms and descriptions of each CT  
147 and MQ trait are presented in Table1.

148

149

150

151           2.3. Slaughter procedure and meat quality parameter measurements

152   The loin muscle (*M. longissimus lumborum*) was removed from the right side of each carcass  
153   included in Exp. 1, vacuum-packed aged for 7 days, and frozen prior to meat quality analysis  
154   at the University of Bristol. Carcasses included in Exp. 2 were subjected to high voltage  
155   electrical stimulation (700 volts RMS for 45 seconds applied between the end of the  
156   processing line and the chiller), chilled and aged for between 7-9 d and dissected, removing  
157   the loin muscle (*M. longissimus lumborum*) from the right side of the carcass. In both Exp. 1  
158   and 2, IMF content was measured in a cross-sectional slice taken from the cranial end of the  
159   muscle at the first lumbar vertebra. Each sample was blended to a fine paste and IMF content  
160   was measured using petroleum ether (B.P. 40-60°C) as the solvent in a modified Soxhlet  
161   extraction (AOAC, 1990). Mean IMF was 1.48% (SD 0.68) and ranged from 0.27 – 3.88%.  
162   The majority of lambs were slaughtered 4-8 d after CT scanning (n=217), and the remaining  
163   lambs were slaughtered 32-33 d after CT scanning (n=160), to allow for a 30 day withdrawal  
164   period from the CT sedative and subsequent taste panel analysis (which formed part of a  
165   wider study). Shear force was also measured, using a TA-XT2 texture analyzer (Stable Micro  
166   System, Surrey, UK) fitted with Volodkevich-type jaws, a standard compression method to  
167   determine tenderness simulating the action of the incisor tooth (Volodkevich, 1938). Loins  
168   were cooked ‘sous-vide’ (in vacuum pack bags) in a water bath at 80°C to an internal core  
169   temperature of 78°C (Teye et al., 2006) monitoring individual loin temperature using a digital  
170   temperature probe (Hanna Instruments UK, Eden Way, Bedfordshire) . Samples were then  
171   immediately cooled in iced water and held at 4°C overnight for a minimum period of 12  
172   hours. Ten 10 x 10 x 20mm samples were cut from each loin following the direction of the  
173   muscle fibers and sheared at a constant speed of 1mm/s perpendicular to the muscle fiber  
174   direction. Shear force was recorded as the force required (kgF) to compress the sample, with



175 greater values for less tender samples. Results were averaged over the ten samples taken from  
176 each loin. Mean shear force was 3.4kgF (SD 1.56) and ranged from 1.39 – 10.72kgF.

177

#### 178 *2.4. Statistical analysis*

179 Lambs with no IMF data were removed (n = 2), lambs without full CT information were  
180 removed (n = 2), and finally lambs with IMF content greater than three standard deviations  
181 from the mean were identified as outliers and also removed (n = 3). Initial regression analysis  
182 and subsequent model checking (Distribution of residuals) suggested the need for  
183 transformation of shear force data. As a result shear force was log-transformed and fitted to a  
184 normal distribution prior to any regression analysis. The number of days from CT scanning to  
185 slaughter (group 1: 4-8 d; group 2: 32-33 d, accounting for lambs subjected to a withdrawal  
186 period to allow subsequent taste panel analysis) was tested using a general analysis of  
187 variance in Genstat14<sup>TM</sup> adjusted for PrCfat, and provided evidence of no significant effect  
188 on IMF content (P = 0.80) or shear force (P = 0.07). The term was also fitted as an  
189 independent variable in the simple regression models in order to test the relationship between  
190 days to slaughter and the CT parameters and was again not significant when tested on IMF (P  
191 = 0.71) and shear force (P = 0.19) therefore was not included in the analysis. A summary of  
192 the CT traits tested in the models are presented in Table 1. Histograms of MQ traits (shear  
193 force prior to transformation and IMF) are presented in Fig. 2.

194

195

196

197

198

199

200 **Table 1:** Acronyms and summary statistics of both CT and meat quality traits along with trait  
 201 descriptions, means and standard deviations (SD) in the Texel data utilized in the prediction  
 202 of IMF (n = 370)

Trait	Acronym	Trait Description	Mean	SD
CT Traits				
	ISCMD	Average muscle density in 2D scan at the ischium (HU)	48.44	2.10
	ISCMSD	SD of muscle density in 2D scan at the ischium (HU)	16.81	0.81
	ISCFD	Average fat density in 2D scan at the ischium (HU)	-62.37	5.32
	ISCFSD	SD of fat density in 2D scan at the ischium (HU)	36.51	2.50
	ISCFA	Carcass fat area measured in 2D scan at the ischium (mm <sup>2</sup> )	3651	1404
	ISCA	Muscle area measured in 2D scan at the ischium (mm <sup>2</sup> )	27415	2898
	TV8MD	Average muscle density in 2D scan at the 8 <sup>th</sup> thoracic vertebra (HU)	44.68	2.98
	TV8MSD	SD of muscle density in 2D scan at the 8 <sup>th</sup> thoracic vertebra (HU)	21.94	1.73
	TV8FD	Average fat density in 2D scan at the 8 <sup>th</sup> thoracic vertebra (HU)	-64.64	5.99
	TV8FSD	SD of fat density in 2D scan at the 8 <sup>th</sup> thoracic vertebra (HU)	39.21	3.16
	TV8FA	Carcass fat area measured in 2D scan at the 8 <sup>th</sup> thoracic vertebra (mm <sup>2</sup> )	3451	1843
	TV8MA	Muscle area measured in 2D scan at the 8 <sup>th</sup> thoracic vertebra (mm <sup>2</sup> )	12380	1833
	ISCSTD	Average soft tissue density in 2D scan at the ischium (HU)	35.55	5.07
	ISCSTSD	SD of soft tissue density in 2D scan at the ischium (HU)	40.34	5.66
	TV8STD	Average soft tissue density in 2D scan at the 8 <sup>th</sup> thoracic vertebra (HU)	21.84	11.35
	TV8STSD	SD of soft tissue density in 2D scan at the 8 <sup>th</sup> thoracic vertebra (HU)	50.56	6.69
	w_md	Average muscle density in the loin spiral scan (weighted by area in each component image) (HU)	46.13	2.22
	w_ms	SD of muscle density in the loin spiral scan (weighted by area in each component image) (HU)	19.91	1.25
	w_fd	Average fat density in the loin spiral scan (weighted by area in each component image) (HU)	-63.97	4.65
	w_fsd	SD of fat density in the loin spiral scan (weighted by area in each component image) (HU)	40.63	3.49
	m_vol	Muscle tissue volume in the loin spiral scan (cm <sup>3</sup> )	1827	281
	f_vol	Fat tissue volume in the loin spiral scan (cm <sup>3</sup> )	298	180
	w_std	Soft tissue density in the loin spiral scan weighted by area (HU)	31.41	8.43
	w_stsd	SD of soft tissue in the loin spiral scan weighted by area (HU)	42.79	6.17
	PrCfat	Predicted total carcass fat weight (kg)	2.34	1.11
MQ Traits				
	Shear force	<i>M. longissimus lumborum</i> shear force (kgF)	3.40	1.56
	IMF	<i>M. longissimus lumborum</i> intra-muscular fat (%)	1.48	0.68

203

204

205 **Insert Figure 2 Here**

206

207 Sixteen models were tested in the analyses (Table 2), termed models A-P using information  
208 from SCTS only (<sup>sp</sup>) and a combination of SCTS and reference information (<sup>com</sup>). Models  
209 with one or two variables included in the maximum model were analyzed using simple and  
210 multiple linear regression, respectively, whilst models employing CT data with more than  
211 two variables were analyzed using stepwise linear regression in Genstat14<sup>TM</sup> (Payne, Murray,  
212 Harding, Baird, & Soutar, 2011), to optimize the number and combination of independent  
213 variables from the maximum fitted model. Models were then tested for significant differences  
214 between correlation coefficients ( $\sqrt{\text{Adj } R^2}$ ) applying standard methods using Fisher's Z  
215 transformation (Mudholkar, 2006). Final models were identified as those with significantly  
216 greater prediction accuracies of MQ traits than the baseline model (Model A). These models  
217 were then validated. During validation, available data were split using a natural time series  
218 separation in the data, as described by Snee (1977). Experiment one data was employed as a  
219 calibration data set, and experiment two data as a validation data set. Summary statistics for  
220 MQ traits and CT measured traits for both calibration and validation data sets are presented in  
221 Table 3, Histograms of MQ traits (shear force prior to transformation and IMF) are presented  
222 in Fig. 3.

223

224

225

226

227

228

229

230

231

232 **Table 2:** Terms included in the maximum linear regression models tested prior to stepwise  
 233 regression using both spiral CT scan parameters only (sp) and spiral CT scan parameters  
 234 alongside two-dimensional reference scan parameters (com). Explanations of acronyms used  
 235 in the models can be found in Table 1

Maximum Models	
SCTS parameters only (sp)	SCTS + 2D reference scan parameters (com)
A PrCfat	PrCfat
B PrCfat, w_md	PrCfat, w_md, ISCMD, TV8MD
C PrCfat, w_fd	PrCfat, w_fd, ISCFD, TV8FD
D PrCfat, m_vol	PrCfat, m_vol, ISCMA, TV8MA
E PrCfat, f_vol	PrCfat, f_vol, ISCFA, TV8FA
F PrCfat, w_md, w_fd	PrCfat, w_md, w_fd, ISCMD, TV8MD
G PrCfat, m_vol, f_vol	PrCfat, m_vol, f_vol, ISCMA, TV8MA, ISCFA, TV8FA
H PrCfat, w_md, w_msd	PrCfat, w_md, w_msd, ISCMD, ISCMSD, TV8MD, TV8MSD
I PrCfat, w_fd, w_fsd	PrCfat, w_fd, w_fsd, ISCFD, ISCFSD, TV8FD, TV8FSD
J PrCfat, w_md, w_msd, w_fd, w_fsd	PrCfat, w_md, w_msd, w_fd, w_fsd, ISCMD, ISCMSD, TV8MD, TV8MSD, ISCFD, ISCFSD, TV8FD, TV8FSD
K PrCfat, w_md, w_msd, w_fd, w_fsd, f_vol	PrCfat, w_md, w_msd, w_fd, w_fsd, f_vol, ISCMD, ISCMSD, TV8MD, TV8MSD, ISCFD, ISCFSD, TV8FD, TV8FSD, ISCFA, TV8FA
L PrCfat, w_md, w_msd, w_fd, w_fsd, m_vol, f_vol	PrCfat, w_md, w_msd, w_fd, w_fsd, m_vol, f_vol, ISCMD, ISCMSD, TV8MD, TV8MSD, ISCFD, ISCFSD, TV8FD, TV8FSD, ISCMA, ISCFA, TV8MA, TV8FA
M PrCfat, w_std	PrCfat, w_std, ISCSTD, TV8STD
N PrCfat, w_std, w_stsd	PrCfat, w_std, w_stsd, ISCSTD, ISCSTSD, TV8STD, TV8STSD
O PrCfat, w_std, w_stsd, f_vol	PrCfat, w_std, w_stsd, f_vol, ISCSTD, ISCSTSD, TV8STD, TV8STSD, ISCFA, TV8FA
P PrCfat, w_std, w_stsd, f_vol, m_vol	Pr_Cfat, w_std, w_stsd, f_vol, m_vol, ISCSTD, ISCSTSD, TV8STD, TV8STSD, ISCFA, ISCMA, TV8FA, TV8MA

236

237 The fitted terms identified in the most accurate prediction models derived from the regression  
 238 analyses using the entire data set were used to produce prediction equations using the  
 239 calibration data set (Exp. 1). These equations were then used to predict MQ traits of the  
 240 lambs included in the independent validation data set (Exp. 2). The coefficient of  
 241 determination ( $R^2$ ) and residual mean square error of prediction (RMSEP) were calculated for  
 242 the predicted MQ traits against chemically extracted IMF and mechanical shear force, to  
 243 identify the simplest and most reliable single predictive model or group of predictive models.

244

245 **Insert Figure 3 Here**

246

247 **Table 3:** Acronyms and summary statistics of both CT and meat quality traits, means and  
248 standard deviations (SD) in the calibration and validation data sets: trait descriptions, means  
249 and standard deviations (SD)

Trait	Acronym	Calibration Data (n=236)		Validation Data (n=134)	
		Mean	SD	Mean	SD
CT Traits					
	ISCMD	49.32	1.78	46.90	1.69
	ISCMSD	16.87	0.76	16.71	0.89
	ISCFD	-63.48	5.59	-60.43	4.14
	ISCFSD	35.89	1.97	37.57	2.97
	ISCFA	3999	1425	3060	1164
	ISCMFA	28328	2486	25823	2887
	TV8MD	44.89	2.98	44.24	2.97
	TV8MSD	21.52	1.68	22.69	1.56
	TV8FD	-64.66	6.58	-64.59	4.84
	TV8FSD	38.48	2.93	40.45	3.18
	TV8FA	3603	1990	3209	1541
	TV8MA	12859	1646	11533	1834
	ISCSTD	35.39	5.45	35.77	4.33
	ISCSTSD	41.77	5.88	37.88	4.23
	TV8STD	21.87	12.25	21.62	9.66
	TV8STSD	50.32	7.41	51.06	5.16
	PrCfat	2.60	1.08	1.88	1.01
	w_md	45.98	2.30	46.40	2.05
	w_msdsd	20.11	1.25	19.55	1.19
	w_fdsd	-64.36	4.41	-63.29	5.01
	w_fsd	40.37	3.46	41.08	3.52
	m_vol	1908	261	1686	259
	f_vol	329	195	244	133
	w_std	30.35	9.18	33.27	6.55
	w_stdsd	43.65	6.57	41.27	5.09
MQ Traits					
	Shear force	3.73	1.69	2.82	1.08
	IMF	1.60	0.79	1.31	0.54

250

251

252 **3. Results**

253 *3.1. Predicting shear force and IMF content using SCTS information*

254 Very little of the variation in shear force was accounted for by PrCfat ( $\text{Adj } R^2 = 0.05$ ),  
255 however PrCfat accounted for a moderate amount of the variation in IMF ( $\text{Adj } R^2 = 0.50$ ).  
256 Compared to the baseline (Model A; Table 2), using only information from CT derived  
257 predicted carcass fat, seven models that included additional CT variables, from the fifteen  
258 models tested, were identified as being statistically significantly more accurate in the  
259 prediction of IMF ( $P > 0.05$ ). None of the additive models using only spiral CT information  
260 were significantly more accurate ( $P < 0.05$ ) in prediction of shear force when compared to the  
261 baseline (Table 4).

262

263 From the seven models identified with significantly increased prediction ability of IMF when  
264 compared to Model A, using only SCTS information, the model with the greatest accuracy  
265 was identified as model L ( $\text{Adj } R^2 = 0.70$ ). This model included CT predicted carcass fat  
266 (PrCfat), weighted muscle density ( $w\_md$ ), fat volume and muscle volume ( $f\_vol$ ,  $m\_vol$ ),  
267 resulting in the prediction equation:

268 " $y = 7.773 + 0.1808 \times PrCfat - 0.1379 \times w\_md + 0.000000881 \times f\_vol -$   
269  $0.0000000338 \times m\_vol$ "

270 The six remaining models including only SCTS information identified as better predictors of  
271 IMF than PrCfat alone were compared with the maximum benchmark (Model L). Models  
272 with significantly reduced accuracy ( $P > 0.05$ ) compared to the benchmark model L were  
273 discarded. This included model P (Table 4), which left a total of six models with correlation  
274 coefficients that were not significantly different, essentially meaning that the prediction  
275 ability of these six models is statistically similar, thus identifying a group of models that  
276 would predict IMF equally using SCTS information. Model K was also dropped as it was

277 entirely the same final model as model J following stepwise linear regression. The final  
278 selected models included; model B ( $\text{Adj } R^2 = 0.67$ ), model F ( $\text{Adj } R^2 = 0.68$ ), model H ( $\text{Adj}$   
279  $R^2 = 0.67$ ), model J ( $\text{Adj } R^2 = 0.69$ ) and model L ( $\text{Adj } R^2 = 0.70$ ).

280

### 281 *3.2. Predicting shear force and IMF content using a combination of SCTS and reference scan* 282 *information*

283 Models using both SCTS information (<sup>sp</sup>) and a combination of SCTS information and  
284 reference information (<sup>com</sup>) were again compared to the simple linear model using only PrCfat  
285 for the predictions of both shear force and IMF. In the analysis for the prediction of shear  
286 force, prediction accuracies were significantly improved with the inclusion of information  
287 from the reference scan images (ISC, TV8). Nonetheless, the overall results show that the  
288 maximum prediction accuracy achieved for shear force, from models developed was  $\text{Adj } R^2 =$   
289  $0.13$  (Table 4).

290

291 In the prediction of IMF ten of the fifteen models tested were significantly greater in  
292 prediction accuracies than that of PrCfat alone ( $P < 0.05$ ). From these models the single ‘best’  
293 model was identified as model L<sup>com</sup> ( $\text{Adj } R^2 = 0.71$ ) and used as a maximum benchmark  
294 model:

$$295 \text{ "y} = 7.675 + 0.3125 * PrCfat - 0.0978 \times w\_md + 0.0000000299 \times m\_vol +$$
$$296 0.000001196 \times f\_vol + 0.0168 \times ISCMD + 0.0371 \times ISCMSD - 0.0000393 \times ISCMA -$$
$$297 0.0543 \times TV8MD + 0.0000236 \times TV8MA - 0.0001298 \times TV8FA"$$

298 Where PrCfat is CT predicted carcass fat, w\_md is weighted muscle density in the spiral  
299 information, m\_vol is the volume of muscle estimated from the spiral information, f\_vol is  
300 the volume of fat estimated from spiral information, ISCMD is the average muscle density in  
301 the ischium scan region, ISCMSD is the standard deviation of muscle density in the ischium

302 scan region, ISCMA is the estimated area of muscle in the ischium scan region, TV8MD is  
 303 the average density of muscle within the 8<sup>th</sup> thoracic vertebra region, TV8MA is the  
 304 estimated muscle area within the 8<sup>th</sup> thoracic vertebra region and TV8FA is the estimated fat  
 305 area within the 8<sup>th</sup> thoracic vertebra region.

306 All models were then tested against the benchmark and any that were statistically  
 307 significantly different in prediction accuracy were discarded ( $P > 0.05$ ), which included  
 308 Model M<sup>com</sup> ( $\text{Adj } R^2 = 0.63$ ). These analyses therefore identified nine “best” models with  
 309 similar prediction abilities: L<sup>com</sup> (benchmark;  $\text{Adj } R^2 = 0.71$ ); F<sup>com</sup>, J<sup>com</sup> and K<sup>com</sup> ( $\text{Adj } R^2 =$   
 310  $0.70$ ); B<sup>com</sup> and H<sup>com</sup> ( $\text{Adj } R^2 = 0.68$ ); O<sup>com</sup> and P<sup>com</sup> ( $\text{Adj } R^2 = 0.67$ ); and N<sup>com</sup> ( $\text{Adj } R^2 =$   
 311  $0.66$ ). Regression results for all models are presented in Table 4.

312 **Table 4:** Regression results for the prediction of ShF or IMF, presented is the adjusted  
 313 coefficient of determination ( $\text{Adj } R^2$ ) and residual mean square error (RMSE) using  
 314 information from SCTS only (sp) or a combination of SCTS and two-dimensional reference  
 315 scans (com), using the whole dataset (n=370).

Model	ShF				IMF			
	sp		com		sp		com	
	Adj $R^2$	RMSE	Adj $R^2$	RMSE	Adj $R^2$	RMSE	Adj $R^2$	RMSE
A	0.03	0.16	0.03	0.16	0.51	0.48	0.50	0.47
B	0.03	0.16	0.07	0.16	0.67**	0.39	0.68**	0.39
C	0.04	0.16	0.05	0.16	0.51	0.48	0.52	0.48
D	0.04	0.16	0.04	0.16	0.56	0.46	0.60	0.43
E	0.03	0.16	0.10*	0.16	0.55	0.46	0.58	0.45
F	0.04	0.16	0.09	0.16	0.68**	0.39	0.70**	0.38
G	0.04	0.16	0.10*	0.16	0.58	0.45	0.60	0.43
H	0.04	0.16	0.09	0.16	0.67**	0.39	0.68**	0.39
I	0.05	0.16	0.09	0.16	0.55	0.46	0.56	0.46
J	0.05	0.16	0.12*	0.16	0.69**	0.38	0.70**	0.37
K	0.05	0.16	0.13*	0.15	0.69**	0.38	0.70**	0.37
L	0.06	0.16	0.13*	0.15	0.70**	0.38	0.71**	0.37
M	0.02	0.16	0.08	0.16	0.54	0.47	0.63*	0.42
N	0.02	0.16	0.09	0.16	0.57	0.45	0.66**	0.40
O	0.03	0.16	0.10*	0.16	0.59	0.44	0.67**	0.40
P	0.04	0.16	0.10*	0.16	0.62*	0.42	0.67**	0.39

316 <sup>sp</sup> Using SCTS information

317 <sup>com</sup> Using a combination of SCTS and reference CT information

318 \*  $\text{Adj } R^2$  differs significantly from the baseline model (A) ( $P > 0.05$ )

319 \*\*  $\text{Adj } R^2$  does not differ significantly from the maximum benchmark model ( $P < 0.05$ )



320 *3.3. Model Validation and selection*

321 Given the poor prediction abilities of CT for shear force ( $R^2 < 0.30$ ) using the parameters  
322 tested, validation analysis for the prediction of shear force was not carried out. Fourteen  
323 possible models in the prediction of IMF were identified. None of these models had  
324 significantly less prediction accuracy ( $P < 0.05$ ) than the single ‘best’ model from both SCTS  
325 information and a combination of SCTS information and reference information (Model L<sup>com</sup>),  
326 so all were retained for validation analyses, with Adj  $R^2$  ranging from 0.67 to 0.71. For  
327 validation, fourteen prediction equations were derived using the calibration data set ( $n = 236$ ),  
328 corresponding to the independent variables identified in the final selected models from the  
329 primary stepwise regression analysis. The models were then used to predict the chemical IMF  
330 values of lambs included in the independent validation data set ( $n = 134$ ). Final validation  
331 results, coefficients of determination ( $R^2$ ) and residual mean square errors of prediction  
332 (RMSEP) are presented in Table 5.

333

334

335

336

337

338

339

340

341

342

343

344

345 **Table5:** Validation results: adjusted coefficient of determination ( $\text{Adj } R^2$ ), residual mean  
 346 square error (RMSE) of calibration; and coefficient of determination ( $R^2$ ) and residual mean  
 347 square error of prediction (RMSEP) of the validation data

Model	Calibration (n=236)		Validation (n=134)	
	Adj $R^2$	RMSE	$R^2$	RMSEP
B <sup>sp</sup>	0.69	0.41	0.60	0.34
F <sup>sp</sup>	0.70	0.41	0.59	0.34
H <sup>sp</sup>	0.69	0.41	0.60	0.34
J <sup>sp</sup>	0.70	0.41	0.62	0.33
L <sup>sp</sup>	0.71	0.40	0.62	0.33
B <sup>com</sup>	0.71	0.40	0.64	0.32
F <sup>com</sup>	0.71	0.40	0.64	0.32
H <sup>com</sup>	0.70	0.40	0.64	0.32
J <sup>com</sup>	0.72	0.40	0.66	0.31
K <sup>com</sup>	0.71	0.40	0.65	0.32
L <sup>com</sup>	0.72	0.39	0.65	0.32
N <sup>com</sup>	0.66	0.43	0.67	0.31
O <sup>com</sup>	0.67	0.43	0.64	0.32
P <sup>com</sup>	0.67	0.42	0.64	0.32

348 <sup>sp</sup> Model uses information from spiral scans only

349 <sup>com</sup> Model uses information from a combination of spiral and two dimensional scans

350

351 The model with the strongest validity was model N<sup>com</sup> ( $R^2 = 0.67$ , RMSEP = 0.31)

352 using both SCTS information and reference scan information, including CT predicted carcass

353 fat (PrCfat), weighted density of soft tissue and its standard deviation (w\_std and w\_stsd) in

354 the spiral scan of the loin, soft tissue density and its standard deviation in the ischium scan

355 (ISCSTD and ISCSTSD), soft tissue density in the 8<sup>th</sup> thoracic vertebra scan and its standard

356 deviation (TV8STD and TV8STSD). This model (N<sup>com</sup>,  $R^2 = 0.67$ ) was then used as a

357 maximum benchmark and the thirteen remaining models also included in the validation

358 analysis were tested against the maximum benchmark using Fisher's z transformation (Rasch

359 et al., 1978). All of the models performed as well as the maximum benchmark model in the

360 validation analysis ( $P < 0.05$ ;  $R^2 = 0.59$  to  $0.66$ ). This left fourteen models for consideration

361 as predictors of IMF, five of which used SCTS information and nine which used a

362 combination of SCTS information and reference information. Details of the final selected

363 prediction models developed from the entire data set are presented in Table 6. These included  
 364 Models B<sup>SP</sup>, F<sup>SP</sup>, H<sup>SP</sup>, J<sup>SP</sup> and L<sup>SP</sup> using SCTS information and models B<sup>com</sup>, F<sup>com</sup>, H<sup>com</sup>, J<sup>com</sup>,  
 365 K<sup>com</sup>, L<sup>com</sup>, N<sup>com</sup>, O<sup>com</sup> and P<sup>com</sup> using a combination of information from both the reference  
 366 scans and SCTS.

367  
 368 **Table 6:** Final prediction models and equations derived from the whole data set, adjusted  
 369 coefficient of determination (Adj R<sup>2</sup>) and residual mean square error of the prediction  
 370 (RMSEP)

Model	Final prediction model equation	Adj R <sup>2</sup>	RMSEP
B <sup>SP</sup>	y=8.048+0.2508*PrCfat-0.1551*w_md	0.67	0.39
F <sup>SP</sup>	y=7.897+0.2347*PrCfat-0.1720*w_md-0.01514*w_fd	0.68	0.39
H <sup>SP</sup>	y=7.10+0.2326*PrCfat-0.1474*w_md+0.0319*w_msd	0.67	0.39
J <sup>SP</sup>	y=7.62+0.1134*Pr_Cfat-0.1566*w_md+0.0401*w_msd-0.02682*w_fd-0.0417*w_fsd	0.69	0.38
L <sup>SP</sup>	y=7.773+0.1808*PrCfat-0.1379*w_md+0.000000881*f_vol-0.000000038*m_vol	0.70	0.38
B <sup>com</sup>	y=8.275+0.2248*PrCfat-0.1113*w_md-0.0490*TV8MD	0.68	0.39
F <sup>com</sup>	y=7.794+0.1704*PrCfat-0.1347*w_md-0.01553*w_fd+0.0183*ISCMD-0.0600*TV8MD-0.00471*TV8FD	0.70	0.38
H <sup>com</sup>	y=7.39+0.2079*PrCfat-0.1043*w_md+0.0298*w_msd-0.0488*TV8MD	0.68	0.39
J <sup>com</sup>	y=6.66+0.1054*PrCfat-0.1138*w_md+0.0661*w_msd-0.02761*w_fd-0.0250*w_fsd-0.0502*TV8MD	0.70	0.37
K <sup>com</sup>	y=5.78-0.1051*w_md+0.0549*w_msd-0.01753*w_fd+0.000000769*f_vol+0.0437*ISCMSD- 0.00703*ISCFD-0.0189*ISCFSD-0.0533*TV8MD	0.70	0.37
L <sup>com</sup>	y=7.675+0.3125*PrCfat-0.0978*w_md- 0.000000299*m_vol+0.000001196*f_vol+0.0168*ISCMD+0.0371*ISCMSD-0.0000393*ISCMA- 0.0543*TV8MD+0.0000236*TV8MA-0.0001298*TV8FA	0.71	0.37
N <sup>com</sup>	y=7.099+0.1101*PrCfat-0.0305*w_std-0.0368*w_std-0.0205*ISCSTD- 0.04523*TV8STD+0.0103*ISCSTSD-0.0404*TV8STSD	0.66	0.40
O <sup>com</sup>	y=7.382+0.2253*PrCfat-0.0251*w_std-0.0332*w_std+0.000001035*f_vol- 0.0322*ISCSTD+0.0142*ISCSTSD-0.04967*TV8STD-0.0387*TV8STSD-0.0001178*ISCFA- 0.0001394*TV8FA	0.67	0.40
P <sup>com</sup>	y=8.554+0.4879*PrCfat-0.0330*w_std-0.0448*w_std+0.000001051*f_vol-0.000000243*m_vol- 0.0000566*ISCMA-0.05713*TV8STD-0.0357*TV8STSD-0.0002859*TV8FA+0.0000371*TV8MA	0.67	0.39

371 <sup>SP</sup> Model uses information from spiral scans only

372 <sup>com</sup> Model uses information from a combination of spiral and two dimensional scans

373

#### 374 4. Discussion

375 It has been demonstrated in previous studies that information from single or multiple CT  
 376 scans can provide moderately accurate predictions of IMF in different sheep breeds.

377 Prediction accuracies range from R<sup>2</sup> = 0.33 to 0.68. (Clelland et al., 2014; Karamichou,

378 Richardson, Nute, McLean, & Bishop, 2006; Lambe, McLean, et al., 2010; J. Macfarlane,  
379 Lewis, Emmans, Young, & Simm, 2006) These studies have provided evidence of the  
380 potential use of single-slice CT scanning as a predictor of IMF in different sheep breeds.

381 The results from this study provide evidence that further improvements in the prediction of  
382 IMF are possible and the use of information from both spiral CT scans and a combination of  
383 spiral CT scans and reference scans can adequately predict intramuscular fat content in the  
384 loin of purebred Texel sheep.

385

386 Prediction models using CT parameters in the assessment of IMF content, achieved a  
387 maximum accuracy of  $\text{AdjR}^2 = 0.70$  and  $0.71$ , using either spiral information only, or a  
388 combination of spiral and reference scan information respectively. The results from this study  
389 indicate that there are several potential prediction models that may be developed, using  
390 different combinations of CT parameters. There was a group of potential prediction models  
391 with increasing degrees of complexity that had similar prediction accuracies for IMF, which  
392 could be indicative of a possible ‘ceiling’ in the achievable prediction accuracies we may  
393 expect using these types of CT parameters. Models that included increasing numbers of  
394 independent variables appeared to be slightly less transferable when validated against the  
395 independent time series data. Although not significant, the models including fewer  
396 independent variables and more direct measures of soft tissue density (average and standard  
397 deviation) were generally more robust during validation. This suggests that the complexity of  
398 the model may have an effect on the accuracy of prediction when applied to an independent  
399 data set.

400

401 Given that there are few, if indeed any, *in vivo* predictors of MQ traits in meat producing  
402 species, prediction accuracies may be acceptable with a suggested lower limit of  $\text{R}^2 = 0.30$ .

403 However in this study the use of CT parameters failed to adequately estimate shear force of  
404 the loin producing an upper limit of  $R^2 = 0.13$ . Similar studies carried out by Lambe et al.  
405 (2008) and Karamichou et al. (2006) reported low phenotypic correlations between two  
406 dimensional CT parameters and shear force ( $r = 0.15 - 0.22$ ,  $r = 0.16$  respectively). Although  
407 IMF is regarded as an important factor in the eating quality of meat when related to mouth  
408 feel, tenderness, juiciness and species-specific flavor, the relationship between shear force  
409 and IMF is less clear. Other factors such as cooking loss, ultimate pH, post-mortem  
410 glycolysis and conditioning (ageing) play an important role in the conversion of muscle to  
411 meat and may have significant effects on shear force results. The CT parameters of the same  
412 muscle *in vivo* to that of a processed, aged and cooked piece of meat may be too far removed  
413 for shear force parameter estimation or prediction to be possible. There is evidence of a linear  
414 relationship between shear force values in cooked meat samples and solvent-extracted IMF  
415 content in raw meat samples and it is generally accepted that this relationship exists  
416 (Hopkins, Hegarty, Walker, & Pethick, 2006; Pannier et al., 2014; Safari, Fogarty, Ferrier,  
417 Hopkins, & Gilmour, 2001), although the size of the effect is often debated.

418 Breeding programs in the UK for several species of livestock have resulted in substantial  
419 genetic improvement in areas such as production efficiency. Genetic improvement in such  
420 traits are permanent and cumulative (Simm, 1998). CT predictions of carcass fat and muscle  
421 weights and muscularity in both the gigot and loin have been used in pedigree UK sheep  
422 breeding programmes over the last two decades (L. Bünger, J.M. Macfarlane, N. R. Lambe, J.  
423 Conington, K. A. McLean, K. Moore, 2011). Together with ultrasound measures of fat and  
424 muscle depth in the loin region, CT measured carcass fat and muscle weights have  
425 contributed much to the success of breeding for leaner carcasses (Moore, McLean, & Bunger,  
426 2011). However, it remains that the drive for reduced carcass fatness and increased  
427 muscularity in current breeding programmes is having an impact on IMF content and as a

428 result meat eating quality traits (Pannier et al., 2014). This study shows that there may be  
429 several approaches using SCTS technology to predict IMF as a MQ trait and a proxy for meat  
430 eating quality traits.

431

432 In conclusion, the prediction of mechanical shear force could not be achieved at an  
433 acceptable level of accuracy employing information from SCTS information, or a  
434 combination of reference scan image information and SCTS information. However, the  
435 prediction of IMF in the loin employing information from SCTS with or without additional  
436 information from reference scans was more promising. This study provides valuable evidence  
437 that the prediction of IMF and related meat eating quality traits for Texel lambs *in vivo* can be  
438 achieved using spiral x-ray CT technology. However the increase in accuracy when  
439 employing SCTS technology was not significant when compared to previous studies using  
440 single slice scanning procedures ( $P < 0.05$ ; Clelland et al., 2014). This suggests that the use  
441 of SCTS technology in the prediction of IMF does not adequately increase prediction  
442 accuracies to justify additional image analysis involved in the processing of the resulting  
443 data. Therefore the authors conclude that although the methods used in this study were  
444 successful in the prediction of IMF, the increased image analysis and processing currently  
445 required does not justify the increase in accuracy achieved when compared to current  
446 reference scan procedures.

447

#### 448 **Acknowledgements**

449 Funding for this work was gratefully received from AHDB Beef and Lamb, Quality meat  
450 Scotland and HCC as part of Neil Clelland's PhD studies. Thanks go to Ian Richardson and  
451 colleagues at the University of Bristol for performing laboratory tests as part of the historical  
452 trials.

453 **References**

- 454 AOAC. (1990). *Official Methods of Analysis* (15th ed.). Association of Official Analytical  
455 Chemists.
- 456 Clelland, N., Bunger, L., McLean, K. A., Conington, J., Maltin, C., Knott, S., & Lambe, N.  
457 R. (2014). Prediction of intramuscular fat levels in Texel lamb loins using X-ray  
458 computed tomography scanning. *Meat Science*, 98(2), 1–9.  
459 <https://doi.org/10.1016/j.meatsci.2014.06.004>
- 460 Font-i-Furnols, M., Brun, A., Tous, N., & Gispert, M. (2013). Use of linear regression and  
461 partial least square regression to predict intramuscular fat of pig loin computed  
462 tomography images. *Chemometrics and Intelligent Laboratory Systems*, 122, 58–64.  
463 <https://doi.org/10.1016/j.chemolab.2013.01.005>
- 464 Glasbey, C., & Young, M. J. (2002). Maximum a posteriori estimation of image boundaries  
465 by dynamic programming. *Applied Statistics*, 51(2), 209–221.
- 466 Hopkins, D. L., Hegarty, R. S., Walker, P. J., & Pethick, D. W. (2006). Relationship between  
467 animal age, intramuscular fat, cooking loss, pH, shear force and eating quality of aged  
468 meat from sheep. *Australian Journal of Experimental Agriculture*, 46(6–7), 879–884.  
469 <https://doi.org/10.1071/EA05311>
- 470 Kalender, W. A. (2006). X-ray computed tomography. *Physics in Medicine and Biology*,  
471 51(13), R29–R43. <https://doi.org/10.1088/0031-9155/51/13/R03>
- 472 Karamichou, E., Richardson, R. I., Nute, G. R., McLean, K. a., & Bishop, S. C. (2006).  
473 Genetic analyses of carcass composition, as assessed by X-ray computer tomography,  
474 and meat quality traits in Scottish Blackface sheep. *Animal Science*, 82(2006), 151–162.  
475 <https://doi.org/10.1079/ASC200518>
- 476 Kongsro, J., & Gjerlaug-enger, E. (2013). In vivo prediction of intramuscular fat in pigs using  
477 computed tomography. *Journal of Animal Science*, 3(4), 321–325.
- 478 L. Bünger, J.M. Macfarlane, N. R. Lambe, J. Conington, K. A. McLean, K. Moore, C. A. G.  
479 and G. S. (2011). Use of X-Ray Computed Tomography (CT) in UK Sheep Production  
480 and Breeding. *CT Scanning-Techniques and Applications, INTECH ...*, 329–348.  
481 Retrieved from [http://www.intechopen.com/books/ct-scanning-techniques-and-](http://www.intechopen.com/books/ct-scanning-techniques-and-applications/use-of-x-ray-computed-tomography-ct-in-uk-sheep-production-and-breeding%5Cnhttp://www.intechopen.com/source/pdfs/20942/InTech-Use_of_x_ray_computed_tomography_ct_in_uk_sheep_production_)  
482 [applications/use-of-x-ray-computed-tomography-ct-in-uk-sheep-production-and-](http://www.intechopen.com/source/pdfs/20942/InTech-Use_of_x_ray_computed_tomography_ct_in_uk_sheep_production_)  
483 [breeding%5Cnhttp://www.intechopen.com/source/pdfs/20942/InTech-](http://www.intechopen.com/source/pdfs/20942/InTech-Use_of_x_ray_computed_tomography_ct_in_uk_sheep_production_)  
484 [Use\\_of\\_x\\_ray\\_computed\\_tomography\\_ct\\_in\\_uk\\_sheep\\_production\\_](http://www.intechopen.com/source/pdfs/20942/InTech-Use_of_x_ray_computed_tomography_ct_in_uk_sheep_production_)
- 485 Lambe, N. R., Macfarlane, J. M., Richardson, R. I., Matika, O., Haresign, W., & Bunger, L.

486 (2010). The effect of the Texel muscling QTL (TM-QTL) on meat quality traits in  
487 crossbred lambs. *Meat Science*, 85(4), 684–690.  
488 <https://doi.org/10.1016/j.meatsci.2010.03.025>

489 Lambe, N. R., McLean, K. A., Macfarlane, J. M., Johnson, P. L., Jopson, N. B., Haresign,  
490 W., ... Bunger, L. (2010). Predicting intramuscular fat content of lamb loin fillets using  
491 CT scanning. In *Proceedings of the Farm Animal Imaging Congress Rennes* (pp. 9–10).

492 Lambe, N. R., Navajas, E. A., Schofield, C. P., Fisher, A. V., Simm, G., Roehe, R., &  
493 Bünge, L. (2008). The use of various live animal measurements to predict carcass and  
494 meat quality in two divergent lamb breeds. *Meat Science*, 80(4), 1138–1149.  
495 <https://doi.org/10.1016/j.meatsci.2008.05.026>

496 Macfarlane, J., Lewis, R., Emmans, G., Young, M., & Simm, G. (2006). Predicting carcass  
497 composition of terminal sire sheep using X-ray computed tomography. *Journal of*  
498 *Animal Science*, 82(3), 289. <https://doi.org/10.1079/ASC200647>

499 Macfarlane, J. M. (2006). Growth, development and carcass quality in meat sheep and the use  
500 of CT scanning as a tool for selection.

501 Mann, A. D., Young, M. J., Glasbey, C. A., & McLean, K. A. (2003). STAR: Sheep  
502 Tomogram Analysis Routines. BioSS.

503 Moore, K., McLean, K. A., & Bunger, L. (2011). The benefits of computed tomography (CT)  
504 scanning in UK sheep flocks for improving carcass composition. In *The British Society*  
505 *of Animal Science and The Association of Veterinary Teaching and Research*.

506 Mudholkar, G. S. (2006). Fisher's Z-Transformation. In *Encyclopedia of Statistical Sciences*.  
507 John Wiley & Sons, Inc. <https://doi.org/10.1002/0471667196.ess0796.pub2>

508 Pannier, L., Pethick, D. W., Geesink, G. H., Ball, A. J., Jacob, R. H., & Gardner, G. E.  
509 (2014). Intramuscular fat in the longissimus muscle is reduced in lambs from sires  
510 selected for leanness. *Meat Science*, 96(2), 1068–1075.  
511 <https://doi.org/10.1016/j.meatsci.2013.06.014>

512 Payne, R., Murray, D., Harding, S., Baird, D., & Soutar, D. (2011). *Introduction to GenStat R*  
513 *for Windows 14th Edition*. VSN International.

514 Prieto, N., Navajas, E. A., Richardson, R. I., Ross, D. W., Hyslop, J. J., Simm, G., & Roehe,  
515 R. (2010). Predicting beef cuts composition, fatty acids and meat quality characteristics  
516 by spiral computed tomography. *Meat Science*, 86(3), 770–779.  
517 <https://doi.org/10.1016/j.meatsci.2010.06.020>

518 Safari, E., Fogarty, N. M., Ferrier, G. R., Hopkins, L. D., & Gilmour, A. (2001). Diverse  
519 lamb genotypes. 3. Eating quality and the relationship between its objective



520 measurement and sensory assessment. *Meat Science*, 57(2), 153–159.  
521 [https://doi.org/10.1016/S0309-1740\(00\)00087-5](https://doi.org/10.1016/S0309-1740(00)00087-5)

522 Simm, G. (1998). *Genetic improvement of cattle and sheep*. Ipswich: Farming Press.

523 Snee, R. D. (1977). Validation of Regression Models: Methods and Examples.  
524 *Technometrics*, 19(4), 415–428. <https://doi.org/10.2307/1267881>

525 Teye, G. A., Sheard, P. R., Whittington, F. M., Nute, G. R., Stewart, A., & Wood, J. D.  
526 (2006). Influence of dietary oils and protein level on pork quality. 1. Effects on muscle  
527 fatty acid composition, carcass, meat and eating quality. *Meat Science*, 73(1), 157–165.  
528 <https://doi.org/10.1016/j.meatsci.2005.11.010>

529 Volodkevich, N. N. (1938). Apparatus for measurements of chewing resistance or tenderness  
530 of foodstuffs. *Journal of Food Science*, 3(1–2), 221–225. [https://doi.org/10.1111/j.1365-](https://doi.org/10.1111/j.1365-2621.1938.tb17056.x)  
531 [2621.1938.tb17056.x](https://doi.org/10.1111/j.1365-2621.1938.tb17056.x)

532

533

534

535

**Figure 1:** Detailed tomogram's, single slice and spiral images produced during CT scanning  
**(a)** First image where TPLV7 appears (i), last image where TPLV1 is no longer visible (ii) and 3D rendered stack of selected images (iii)  
**(b)** Scan image from ischium region (i) and scan image from 8<sup>th</sup> thoracic vertebra region (ii)

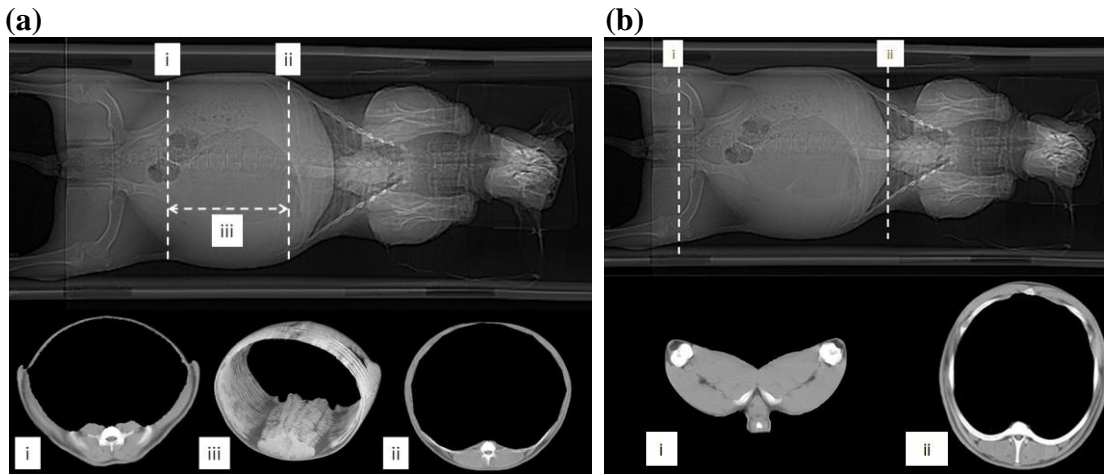


**Figure 2:** Histograms of chemically extracted intramuscular fat percentage (IMF %) and shear force (kgF) measured in the loin of the Texel lambs (n = 370)

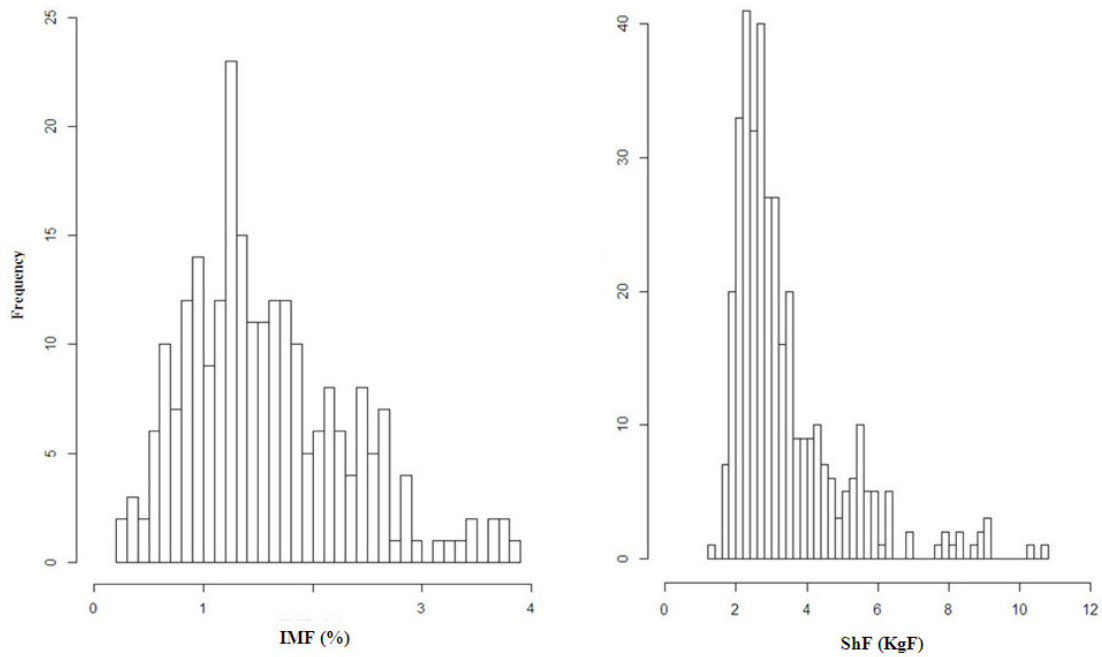
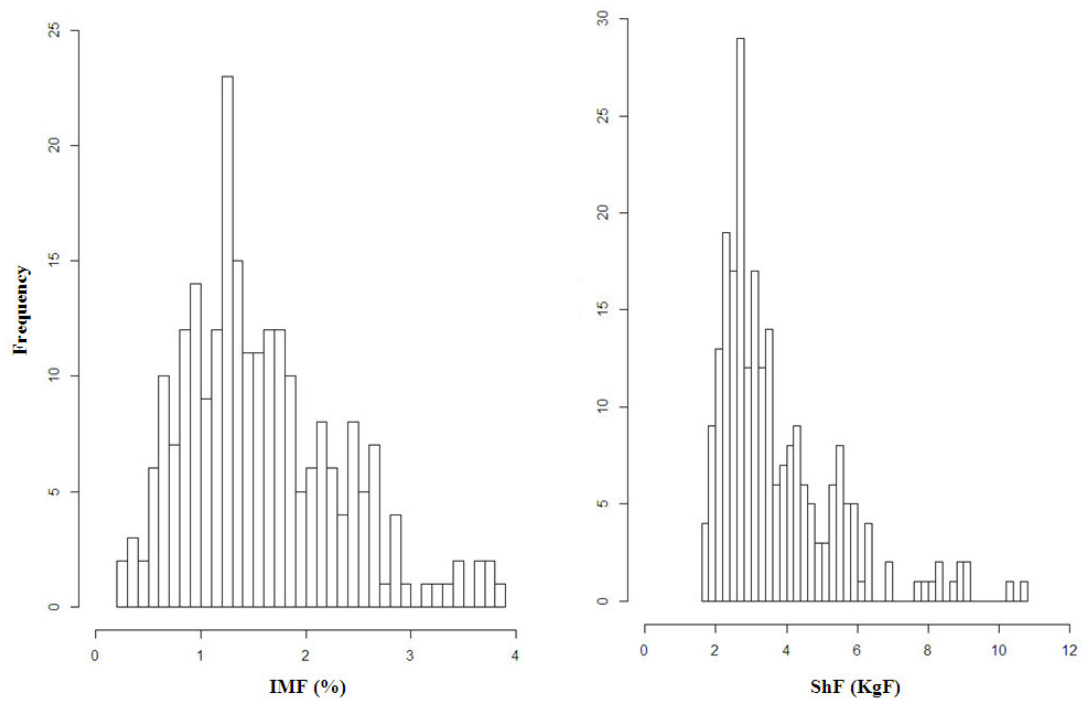


**Figure 3:** Histogram of chemically extracted intramuscular fat percentage (IMF %) and shear force (kgF) both measured in the loin in the calibration and validation data sets

Calibration (n=236)



Validation (n=134)

